

**Large-scale Computational Polymer Solubility Predictions  
and Applications to Dissolution-based Plastic Recycling**

Journal:	<i>Green Chemistry</i>
Manuscript ID	GC-ART-02-2023-000404.R2
Article Type:	Paper
Date Submitted by the Author:	27-Apr-2023
Complete List of Authors:	Zhou, Panzheng; University of Wisconsin System, Chemical and Biological Engineering Yu, Jiuling; University of Wisconsin-Madison, Department of Chemical and Biological Engineering Sánchez-Rivera, Kevin; University of Wisconsin-Madison, Chemical and Biological Engineering Huber, George; University of Wisconsin, Chemical and Biological Engineering Van Lehn, Reid; University of Wisconsin-Madison, Chemical and Biological Engineering

# Large-scale Computational Polymer Solubility Predictions and Applications to Dissolution-based Plastic Recycling

*Panzheng Zhou, Jiuling Yu, Kevin L. Sánchez-Rivera, George W. Huber, and Reid C. Van Lehn\**

Department of Chemical and Biological Engineering, University of Wisconsin – Madison, Madison, WI, 53706, United States.

\*send correspondence to: [vanlehn@wisc.edu](mailto:vanlehn@wisc.edu)

## **Abstract**

Dissolution-based plastic recycling is a promising approach to separate and recover high quality pure polymer resins from multicomponent plastic waste by exploiting differences in polymer solubility. The design of a dissolution-based polymer recycling process requires the selection of appropriate solvent systems and operating temperatures to dissolve only target polymers. Determining these parameters experimentally is challenging due to the wide range of solvents and temperatures possible for a given set of target polymers. In this work, we report a computational scheme that employs molecular dynamics simulations and the Conductor-like Screening Model for Realistic Solvents to predict polymer solubilities. Using this scheme, we established a computational solubility database for 8 common polymers and 1007 solvents at multiple temperatures and measured selected solubilities experimentally to validate computational predictions. Analysis of functional groups within this large database then provides chemical heuristics relating the molecular structures of good and non-solvents for selected polymers. We further developed a tool that automates the selection of solvents for all possible sequences in which target polymers can be selectively dissolved to guide the design of dissolution-based plastic recycling processes. We demonstrate the application of these methods via multiple experimental case studies of representative dissolution-based polymer recycling processes in which pure polymer resins were successfully recovered from physical mixtures of polymers.

## Introduction

Seven billion tons of plastic waste have been generated globally to date, but less than 10% of these materials has been recycled.<sup>1</sup> The estimated annual loss due to plastic packaging, which is the largest constituent of plastic waste, during sorting and processing alone is 80-120 billion dollars.<sup>2</sup> A key factor that contributes to the low rate of plastic recycling is that current plastic recycling technologies are mostly designed for single-component plastics and are unable to deal with multicomponent plastics due to their complex compositions and the incompatibility of different polymers.<sup>3-5</sup> For example, multilayer plastic films are widely used in the packaging industry and over 100 million tons are produced worldwide each year.<sup>6,7</sup> These films are made of several layers of different polymers that each contributes useful functional properties (*e.g.*, mechanical stiffness, barrier properties).<sup>8-10</sup> However, the concomitant heterogeneity of such multicomponent materials hinders their recycling.<sup>11</sup> As a result, while over 29% of some single-component plastic bottles was recycled in the U.S. in 2018, only 8.7% of all plastic municipal solid waste was recycled and most multilayer films are diverted to landfills.<sup>12</sup>

A promising, near-term approach to recycle multicomponent plastics is dissolution-based polymer recycling. In this approach, differences in polymer solubility permit the separation and recovery of pure polymer resins from carefully chosen solvent systems that dissolve only target polymers.<sup>11, 13</sup> Dissolution-based plastic recycling has several advantages over chemical or mechanical recycling methods: it can process multicomponent plastic mixtures, it maintains the chemical structures and properties of recovered polymers, and it does not require a high-purity input stream because impurities and additives can be removed by selective dissolution.<sup>14-18</sup> Dissolution-based recycling is also a green process that has over 40% lower greenhouse gas emissions than producing virgin resins, saving 3-6 tons CO<sub>2</sub> for each ton of plastic waste.<sup>19</sup> In addition, dissolution-based technologies can reduce emissions to an extent comparable to closed-loop mechanical recycling, and have 65-75% less environmental impact than incineration.<sup>16, 20, 21</sup> Recently, we proposed a dissolution-based process called Solvent-Targeted Recovery and Precipitation (STRAP) to recycle multilayer plastic films.<sup>11, 22</sup> In STRAP, a suitable solvent selectively dissolves a target polymer from the multilayer film at a defined temperature, the mixture is filtered to separate the dissolved polymer from the residual film components, and the polymer is precipitated and recovered by adding non-solvent (a solvent in which the polymer is insoluble) and/or decreasing the temperature. This process is then repeated sequentially for each target polymer until all resins have been recovered from the film. We have demonstrated the recovery of high-density polyethylene (HDPE), ethylene vinyl alcohol (EVOH), and polyethylene terephthalate (PET) resins from post-industrial waste films via STRAP.<sup>11, 22, 23</sup> We have previously performed process simulations and life-cycle assessment to demonstrate the environmental benefits of STRAP processes. For example, a STRAP process that recycles PE, EVOH and PET from a multilayer plastic film generates 54% fewer emissions than producing the virgin films.<sup>17, 22</sup> Some dissolution-based plastic recycling technologies are also being developed industrially, although limited information about their process conditions and solvent selections is openly available.<sup>5, 13, 16</sup> These processes highlight the feasibility and broad applicability of recycling polymers from complex input streams via dissolution-based approaches.

The design of a successful dissolution-based polymer recycling process requires the selection of an appropriate solvent (and non-solvent in some cases) for each polymer of interest, temperatures for dissolution and precipitation, and the amount of solvent. These considerations affect the efficiency, economics, and environmental impact of the process.<sup>17, 22</sup> The key

information needed to guide these choices is the temperature-dependent solubilities of polymers in different solvent systems. Several past studies have reported known solvents and non-solvents for some common polymers at various temperatures;<sup>24, 25</sup> examples are included in Table S1 of the ESI. However, solvent selection for complex input streams containing multiple polymers often requires consideration of a broader range of possible solvents, and the experimental collection of polymer solubility data at a large scale is prohibitively time-consuming. Alternatively, computational methods can enable effective, large-scale solvent screening which can be valuable for process design as well as for evaluating alternative sets of solvents based on cost, sustainability, or toxicity. For example, tabulated solubility parameters are often used to identify possible solvents/non-solvents for a given polymer with minimal computational effort. Examples of solubility parameters include Hildebrand,<sup>26</sup> Hansen,<sup>27</sup> Kamlet-Taft,<sup>28</sup> Gutmann,<sup>29</sup> and Swain<sup>30</sup> parameters. In particular, Hansen solubility parameters (HSPs) are widely used to guide solvent selection for polymers because tabulated HSP values are available for a great number of solvents and polymers. There are many successful applications of solvent screening with HSPs.<sup>27, 31</sup> Machine learning methods have also been developed for solvent selection. For example, a recent study trained a deep neural network for binary solvents/non-solvent classification with over 4500 homopolymers and 24 common solvents with an accuracy of 93.8%.<sup>32</sup> While valuable, these prior computational methods generally focus on qualitatively distinguishing good and non-solvents for a given polymer at room temperature as opposed to quantitatively predicting solubility as a function of temperature. These drawbacks limit their applicability to the design of dissolution-based processes, which require quantitative values of polymer solubility (to determine the amount of solvent needed) as a function of temperature (to determine operating temperatures). Another challenge with HSPs is uncertainty in the selection of HSPs for specific polymer resins, as detailed further in the ESI. The lack of computational methods to predict temperature-dependent polymer solubilities in a wide range of solvents, and for specific polymer resins, is thus the gap that we seek to address.

In this work, we address this gap by using molecular-scale models to generate quantitative, temperature-dependent, and large-scale solubility predictions for 8 common polymers in 1007 solvents at multiple temperatures.<sup>11, 33</sup> Our approach utilizes classical molecular dynamics (MD) simulations to sample representative oligomer conformations as input for Conductor-like Screening Model for Real Solvents (COSMO-RS) solubility calculations, which are calibrated by an experimentally measured solubility for each polymer in a reference solvent. We perform such solubility predictions for polymers that are common components of plastic waste, including EVOH, PE, PET, polypropylene (PP), polystyrene (PS), polyvinyl chloride (PVC), nylon 6 and nylon 66. Experimental measurements are subsequently performed to validate the computational predictions. Using this database, we provide chemical insights into solvent preferences for polymers based on functional group analysis. We then show how computational tools can aid the design of STRAP processes by evaluating feasible solvents for all possible separation sequences (*i.e.*, sequences of successive solvent washes, each designed to selectively dissolve a single target polymer) for systems representative of multicomponent plastic waste. Specifically, we demonstrate the applicability of the computational methods through the successful experimental separation of three different physical mixtures of polymers (PE/PS, PVC/PET, and PP/EVOH/PET) via multiple separation sequences. These computational methods have the ability to rapidly guide the design of dissolution-based plastics recycling processes to accelerate their application to new waste

feedstocks and have the potential to identify green solvents as replacements for solvents utilized in existing selective dissolution processes.<sup>22, 33-35</sup>

## Methods

### Summary of approach

Our approach employs a series of computational methods to predict polymer solubilities in conjunction with experimental measurements of solubility for calibration and validation. This workflow is designed to address limitations with conventional solvent selection based on HSPs, which cannot provide quantitative predictions of polymer solubility as a function of temperature. Another challenge with HSPs addressed by our approach is the potential uncertainty when selecting specific HSP values for a given resin (as further discussed in the ESI). Like predictions based on HSPs, our approach does not explicitly use resin molecular weight or crystallinity as inputs for solubility predictions; however, we do use experimental input to calibrate the model, thereby accounting for these resin-specific properties. Further discussion comparing our approach to existing methods is included in the ESI.

**Figure 1** summarizes the general workflow for solubility predictions and the application of these predictions to STRAP processes in 5 steps:

1. Using the molecular structure of the chosen polymer (modeled as an oligomer) and solvent, perform an MD simulation of a single oligomer in dilute solution to obtain a simulation trajectory that samples a wide range of chain conformations.
2. Select a set of conformers from the MD trajectory to span a range of representative oligomer structures.
3. Based on the selected conformers and a reference experimentally measured solubility for the target polymer, perform COSMO-RS solubility calculations to establish a polymer solubility database.
4. Verify selected values from the database with experimental measurements.
5. Based on the predicted solubilities, identify selective solvents for STRAP processes for plastic waste that contains multiple polymers. Test the proposed polymer recycling process by using model systems consisting of physical mixtures of polymers.

The computational solubility database established via this approach contains 8 common polymers (EVOH, PE, PP, PS, PET, PVC, nylon 6, and nylon 66) and 1007 solvents. We then demonstrate the STRAP polymer recycling processes for 3 different physical mixtures of polymers (PE/PS, PVC/PET, and PP/EVOH/PET) which are common components of multilayer films. Details of the specific methods for each step are described in the following sections.

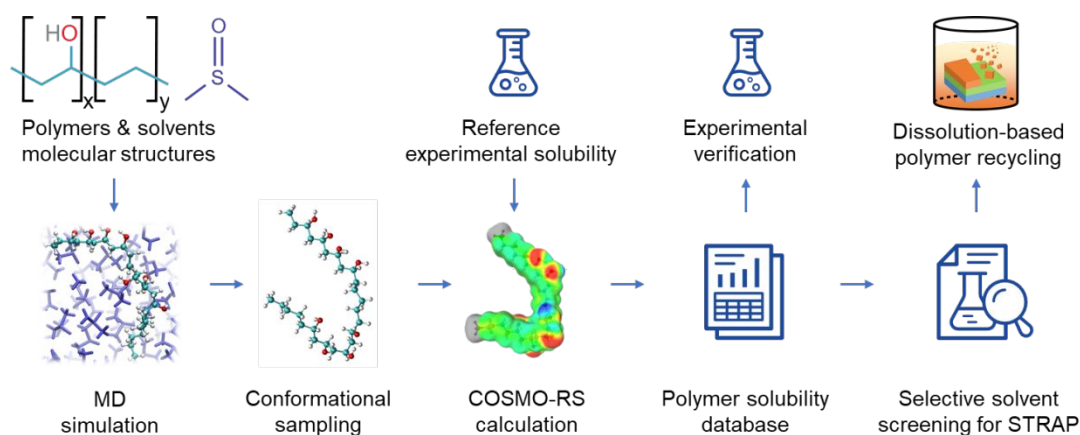


**Figure 1.** Summary of computational and experimental approach for large-scale polymer solubility prediction, validation and application.

### Computational simulations for solubility prediction

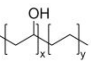
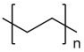
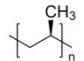
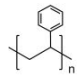
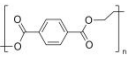
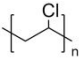
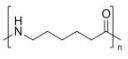
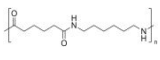
We first model the polymers as oligomer molecules and perform MD simulations of these oligomers in dilute solutions to obtain trajectories of representative oligomer conformations, following the workflow established in our previous work.<sup>33</sup> **Table 1** shows detailed information on the polymer structures and number of monomers included in the corresponding oligomers. Atomistic MD simulations were performed in the isothermal-isobaric ensemble using *Gromacs 2016*.<sup>36</sup> Each MD simulation contained 1 oligomer molecule and 216 solvent molecules. Solvents were selected for these simulations based on literature reports of good solvents for the target polymers.<sup>24, 25</sup> Specifically, EVOH was simulated in dimethyl sulfoxide (DMSO); PE, PP and PS were simulated in toluene; PVC and PET were simulated in dichloromethane; and nylon 6 and nylon 66 were simulated in tetrahydrofuran (THF). All molecules were parameterized using Antechamber and the Generalized AMBER force fields.<sup>37, 38</sup> The simulation system was initialized with a cubic box containing a single polymer. The system was then solvated, energy minimized, and equilibrated for 2 ns in an *NPT* simulation at 300 K and 1 bar using a velocity-rescale thermostat and Berendsen barostat. A 10 ns *NPT* simulation was then performed at the same temperature and pressure using the Nosé-Hoover thermostat and Parrinello-Rahman barostat. All simulations were performed using a leapfrog integrator with a 2-fs timestep. Verlet lists were generated using a 1.2 nm neighbor list cutoff. Van der Waals interactions were modeled with a shifted Lennard-Jones potential and Verlet cutoff-scheme that was smoothly shifted to zero at 1.2 nm. Electrostatic interactions were calculated using the smooth Particle Mesh Ewald method with a short-range cutoff of 1.2 nm, grid spacing of 0.14 nm, and 4<sup>th</sup> order interpolation. Bonds were constrained using the LINCS algorithm. All thermostats used a 2.0 ps time constant and all barostats used a 2.0 ps time constant with an isothermal compressibility of  $3.0 \times 10^{-5} \text{ bar}^{-1}$ .

We then sampled representative oligomer structures (referred to as conformers) from the MD trajectories based on two structural parameters: the radius of gyration ( $R_g$ ) and the solvent-accessible surface area (SASA). Sampling conformers that cover a range values of these two parameters can provide reliable input for COSMO-RS solubility estimations.<sup>33, 39</sup> We thus selected conformers by superimposing a square grid over the two-dimensional  $R_g$ -SASA scatter plot and choosing conformers closest to grid intersections following our previous work.<sup>33</sup> The number of sampled conformers for each polymer is listed in **Table 1**. The selected

conformers were input to density functional theory (DFT) calculations to obtain screening charge densities (COSMO files). The DFT calculations included a geometry optimization in implicit water using the conductor-like polarizable continuum model and a single-point calculation in the infinite dielectric constant limit. These DFT calculations were performed with *Gaussian 16* at the BVP86/TZVP/DGA1 level of theory.<sup>40</sup> Precalculated COSMO files for the solvents were obtained from the database *COSMObase-1901-BP-TZVP*.

COSMO files from the DFT calculations were input to COSMO-RS for solubility calculations. COSMO-RS predicts the thermodynamic properties of multicomponent systems based on quantum mechanical calculations and statistical thermodynamics methods.<sup>41, 42</sup> The chemical properties of each molecule are represented by the probability distribution of the screening charge densities (called the  $\sigma$ -profile).  $\sigma$ -profiles of all oligomer conformations with deactivated terminal groups were used to approximate the  $\sigma$ -profile of the corresponding polymer.<sup>43</sup> The  $\sigma$ -profiles were then used to calculate the chemical potential of the polymer to enable predictions of solubility via a solid-liquid equilibrium calculation.<sup>44</sup> This calculation requires the polymer melting temperature and an experimentally measured solubility as reference input. **Table 1** shows the reference experimental solubilities used in this work (measured following the methods described below). Melting temperatures were taken from literature sources.<sup>45, 46</sup> All COSMO-RS calculations were performed using the *COSMOtherm 19* software with the BP\_TZVP\_19 parameterization.<sup>47-49</sup>

**Table 1.** Modeling information and reference experimental input for each polymer.

Polymer	Modeling information	Number of conformers	Reference experimental input		
			Solvent	T (°C)	Solub (wt%)
EVOH 	6-mer (4VA:2E), random copolymer structure	24	DMSO	95	19.4
PE 	6-mer	31	Toluene	110	23.1
PP 	6-mer, isotactic	25	Toluene	110	31.2
PS 	6-mer, atactic	29	Toluene	110	41.2
PET 	4-mer	22	DMSO	135	13.3
PVC 	6-mer, atactic	27	THF	50	14.9
Nylon 6 	4-mer	20	Acetic acid	90	10.8
Nylon 66 	2-mer	28	DMSO	135	3.1

### Experimental solubility measurements and polymer separations

Experimental solubility measurements for all eight polymers in multiple solvents were performed to calibrate and validate the computational solubility predictions. PP (isotactic, weight-average molecular weight ~12,000, number-average molecular weight ~5,000) and PVC (high molecular weight) were purchased from Sigma-Aldrich (St. Louis, Missouri, USA). PS was purchased from Goodfellow Cambridge Ltd. (Huntingdon, UK). Low density PE (DOW™ 608A), EVOH (32 mol% ethylene content, CCP EV3251), PET (DAK Americas Laser+® C 9921), nylon 6 (BASF Ultramid® B36), and nylon 66 (DuPont Zytel® FG42A) resins were purchased and provided by Amcor Flexibles. These resins were selected because they are used commonly in industry and by major manufacturers.<sup>11, 22</sup> Consequently, we expect their solubilities to be representative of the solubilities of components of common commercial plastic materials. Each polymer was separately dissolved in a reference solvent to support the creation of the computational solubility database. To validate computational predictions, each polymer was also dissolved in predicted good and non-solvents.

Experiments to measure individual polymer solubilities were performed in a three-necked 100 mL round bottom flask which was equipped with a reflux condenser, a thermometer, and a glass stopper. Approximately 40 g solvent and a magnetic stir bar were put into the flask, which was then immersed in a 1000 mL silicon oil bath with continuous agitation and heated to the target temperature. When the target temperature was reached, 1 wt% (with respect to the solvent mass) of polymer resin was added into the heated solvent and the solvent and polymer were stirred for 0.5 h to permit dissolution. If the polymer resin dissolved completely, another 1 wt% of polymer resin was added, and the above process was repeated until no further resin could be dissolved after 0.5 h mixing. The undissolved resin was filtered from the solvent, washed with DI water, dried in a vacuum oven at 100 °C for 3 h, and weighed to determine its mass after drying. The solubility was then computed as shown in Equation 1.

$$\text{Solubility (wt\%)} = \frac{\text{Added polymer mass} - \text{undissolved polymer mass}}{\text{mass of solution}} \times 100\% \quad (\text{Eq 1})$$

It should be noted that for some polymer resins, the solubility is regarded as a lower limit because the high viscosity of the solution at the measured value inhibited further dissolution. More details regarding experimental procedures are available in the ESI.

Physical mixtures of polymers were experimentally separated by sequential dissolution to show the feasibility of our polymer separation strategies. Three polymer mixtures were studied, including a PE/PS mixture, PET/PVC mixture, and PP/EVOH/PET mixture. Around 3 g of the desired mixtures (with a 1:1 mass ratio for the 2-component mixtures and 1:1:1 mass ratio for the 3-component mixture) were added into ~30 g of the selected solvents in a round bottom flask and heated to the desired temperature under stirring using a 1000 mL silicon oil bath. After 1 h dissolution, the flask was removed from the oil bath and emptied into a 250 mL beaker using a hot stainless wire cloth as the filter. The undissolved polymer was collected from the surface of stainless wire cloth and washed with DI water. A same amount of the non-solvent (if applicable) was added into the beaker to precipitate the dissolved polymer. The precipitated polymer was filtered with a Büchner funnel. Both dissolved and undissolved polymers were dried at 100 °C for 3 h in a vacuum oven. The mass balance was calculated based on the mass of dried polymers. For the 3-component mixture, the aforementioned dissolution step was repeated twice with different solvents.



## Results and Discussion

### Creation of the polymer solubility database

We developed a database of computationally predicted polymer solubilities following the approach detailed in the Methods section. We modeled polymers as short oligomers, performed MD simulations of these oligomers in dilute solution to obtain various chain configurations, selected 20-31 conformers from the MD trajectories for each polymer (**Table 1**), and calculated screening charges for each of these conformers.<sup>33</sup> **Figure 2** shows some example conformers sampled from the MD simulations following this approach and their corresponding screening charge densities. Screening charge densities serve as the input to solid-liquid equilibrium calculations using COSMO-RS to evaluate polymer solubilities in various solvents. Solubilities were calculated for each polymer-solvent system at room temperature (RT) and a higher temperature (Th) because solubilities generally increase with temperature. The higher temperature is determined by the boiling point of the solvent: if the boiling point is greater than 120 °C, Th = 120 °C; otherwise, Th was selected as the temperature 1 °C lower than the boiling point. The upper bound on temperature enables calculations of polymer solubility at elevated temperatures while avoiding temperatures that are too high, which may lead to melting or thermal degradation and thereby influence the properties of the recovered materials.<sup>45, 50</sup> Using this approach, we performed large-scale solubility predictions for 8 polymers and 1007 solvents at both temperatures, establishing a solubility database with over 16,000 data points. **Table 2** shows some selected results from these solubility predictions for 25 common polymer-solvent systems. The complete database is available in the ESI.

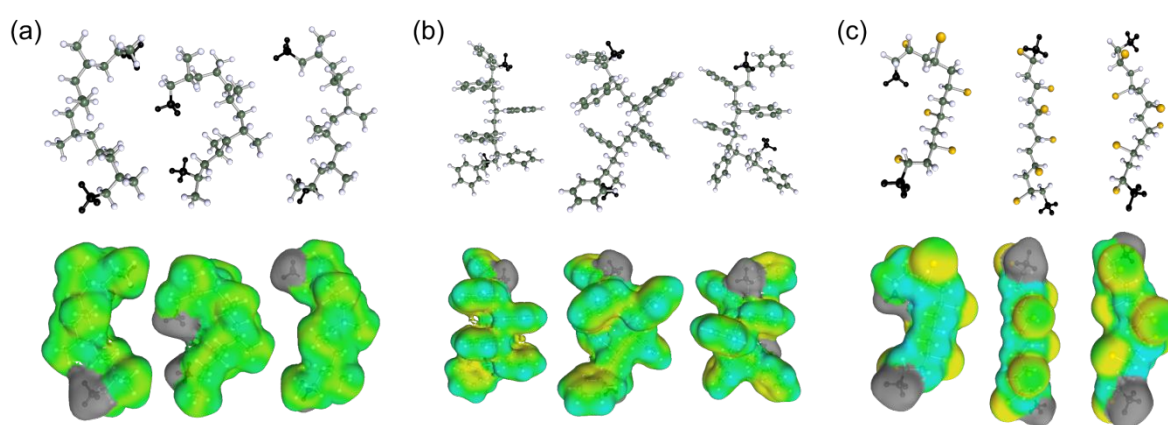


**Figure 2.** Some structures obtained from conformational sampling and corresponding COSMO-RS representations (colored surfaces) for 3 polymers: (a) PP, (b) PS, and (c) PVC. End groups of these oligomer molecules (black atoms) are neglected in the COSMO-RS calculations (gray surfaces) to represent the chemical properties of longer polymer chains.

To verify the computational predictions, we conducted experimental measurements to determine polymer solubilities in one predicted good solvent and one predicted non-solvent for each polymer. We define good solvents of a polymer as solvents with predicted solubilities > 3 wt% and non-solvents as those with predicted solubilities  $\leq$  3 wt%. For the experiments, we prioritized common laboratory solvents to avoid concerns of toxicity or safety.<sup>33</sup>

**Table 2.** Selected results from the solubility database. Each polymer-solvent system is studied at a room temperature (RT) and a higher temperature (Th). Th is set as 1 °C lower than the boiling point of the solvent with an upper bound of 120 °C.

Solvent	Boiling point (°C)	Predicted polymer solubility (wt%)									
		EVOH		PE		PET		PS		PVC	
		RT	Th	RT	Th	RT	Th	RT	Th	RT	Th
Methanol	64.6	0.0	0.8	0.0	0.1	0.0	0.0	0.0	0.0	0.1	0.8
Toluene	110.6	0.0	0.3	0.1	22.6	0.0	2.5	3.6	41.0	0.7	14.8
THF	65	0.1	0.9	0.1	1.7	0.0	0.8	14.0	31.3	8.9	19.1
Water	100	0.0	0.0	0.0	0.0	0.0	0.0	0.0	0.0	0.0	0.0
Benzene	80	0.0	0.0	0.0	3.1	0.0	0.9	5.3	29.3	1.0	8.1

**Table 3** summarizes the polymer-solvent systems and compares solubilities measured experimentally and predicted computationally. There are 2 experiments (nylon 6 and nylon 66 in DMF) for which accurate solubilities could not be measured due to the retention of the (good) solvent in the polymer. These values thus qualitatively support the prediction of high solubility, but numerical solubilities are not provided in the table. Among the 14 systems that have available experimental data points, 11 of them demonstrate good agreement between computations and experiments with the average absolute difference between predicted and experimental solubilities equal to 1.3 wt%. Two systems (PP in THP and PS in THF) have acceptable accuracy, as the computational predictions correctly identify good/non-solvents but exhibit some deviations from experimental data. Only 1 system (PET in DMF) has a computational result that is qualitatively inconsistent with the experiment. In this system, DMF was predicted to be a good solvent for PET but proved to be a non-solvent experimentally. However, we note that PET is known to be challenging to dissolve and that it is possible that kinetic effects associated with a slow rate of dissolution could inhibit accurate solubility measurements.<sup>51,52</sup> Overall, the experimental verification of the database identified 11/14 good, 2/14 acceptable, and 1/14 incorrect predictions. This overall good agreement between computational and experimental solubilities validates the suitability of the solubility database for further investigation.

**Table 3.** Experimental verification of solubility predictions. The solubility of each polymer is measured in a good solvent and a non-solvent (distinguished by a threshold of 3 wt% in predicted values). Among the 14 available test results, 11 computational predictions are in good agreement with experimental data (denoted by the green color), 2 predictions are acceptable as they correctly identify good/non-solvents but have some deviations in solubility values (yellow color), and 1 prediction is inconsistent with experiment (red color).

Polymer	Good solvent	T (°C)	Pred solub (wt%)	Expt solub (wt%)	Non-solvent	T (°C)	Pred solub (wt%)	Expt solub (wt%)
EVOH	DMF	120	30.8	27.3	acetone	55	0.2	0
PE	dodecane	120	32.5	30.1	acetone	55	0.3	0
PP	THP	87	20.9	6.4	acetone	55	1.4	0
PS	THF	25	14.0	24.4	2-propanol	82	1.2	0.01
PET	DMF	120	18.4	0.5	acetone	55	0.7	0.01
PVC	THP	87	17.9	14.7	ethylene glycol	122	1.6	< 0.46
Nylon 6	DMF	120	7.3	*	acetone	55	0.2	0.01
Nylon 66	DMF	120	4	*	acetone	55	0.1	0.01

\*data unavailable due to solvent retention

### Analysis of polymer solubility trends

Based on the large-scale solubility prediction results, we next analyzed the complete set of solvents to identify sets of good and non-solvents for each polymer by rank-ordering predicted solubilities. To provide heuristics regarding the feasibility of dissolving different polymers, we first defined a set of “top” solvents for each polymer. Here, we define the top solvents as the top 5% of all solvents ranked by solubility. The statistics of these solvents gives a general idea of the difficulty to dissolve each polymer. **Figure 3** shows the distributions of polymer solubilities in their top solvents at room temperature and at elevated temperatures. As expected, polymer solubilities are mostly low at room temperature and increase at higher temperatures. Accordingly, dissolution-based recycling processes typically dissolve the resins in a heated solvent and precipitate in a cooled system.<sup>22</sup> For example, **Figure 3** indicates that there are very few good solvents for PE at room temperature but such solvents are easy to identify at higher temperatures. As a comparison, PET, nylon 6 and nylon 66 have relatively low solubilities even in their high-temperature top solvents. This comparison indicates that the dissolution of PET and nylons can be challenging in general, and if possible, dissolution-based recycling processes should be designed to avoid dissolving these components. Indeed, we have recently developed STRAP processes for multilayer plastic films containing PET which was often the last in the separation sequence and thus was recovered as a residual solid without being dissolved.<sup>11, 22</sup>

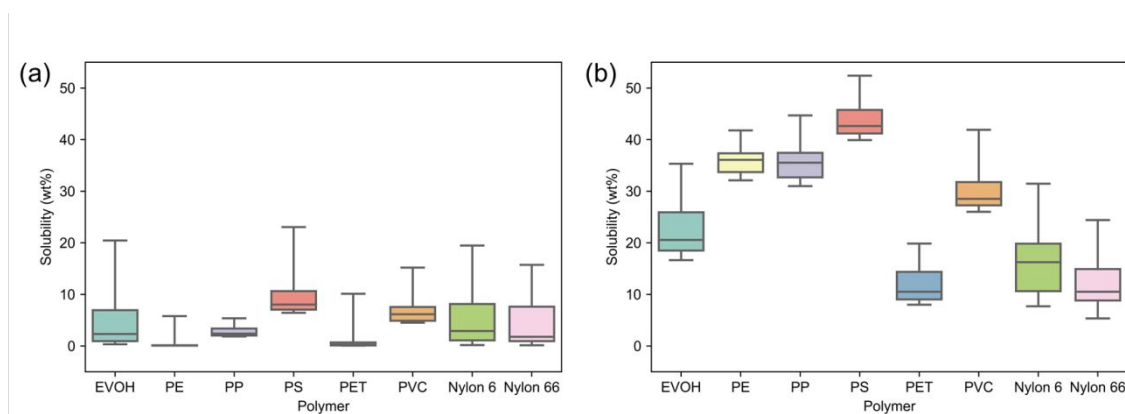


**Figure 3.** Polymer solubilities in their top 5% solvents at (a) room temperature (b) and elevated temperatures. The dataset for each polymer is displayed as a box plot, which contains five horizontal lines that represent the minimum, lower quartile, median, upper quartile, and the maximum values. The box denotes the range from lower quartile to higher quartile, which is the middle half of the dataset.

The solubility database can also provide chemical heuristics on polymer dissolution. To study the general relationship between the molecular structures of polymers and solvents, we analyzed the occurrence of different functional groups in the top solvents of each polymer. For this comparison, we define the top solvents of a polymer as those within the top 10% of all solvents ranked by solubility while also having a minimum solubility of 5 wt% at any temperature. The 5 wt% threshold is to guarantee that the set of top solvents only includes solvents with appreciable solubility values. We then performed functional group analysis for these solvents based on their molecular structures and assign each solvent to one or more classes based on their functional groups. For example, toluene is considered to be part of the “aromatic” class and glycol is considered part of the “alcohol” class. This analysis was performed with SMILES string representation of molecules and SMARTS substructure matching syntax via RDKit.<sup>53-55</sup>

**Table 4** summarizes the analysis of top solvent classes. We first notice that the sets of top solvents for these polymers can include a different number of solvents. PET, nylon 6 and nylon 66 have fewer top solvents than the other polymers, indicating that the dissolution of these three polymers is generally more challenging, which is consistent with our observations of **Figure 3**. The table also lists the top solvent classes and example solvents for each polymer. Solvent classes are sorted by what percentage of the top solvents are in each class; only solvent classes that represent at least 10% of the top solvents are listed in **Table 4**. The list of functional groups aligns with our chemical intuition of “like dissolves like” as many top solvent classes share the same functional groups with the polymers. For example, alcohol is the most common solvent class for EVOH, which is a polymer with hydroxy groups; alkane and alkene are top classes for PE and PP; and aromatic compounds are the best for PS and PET. These solvent class rankings provide a general solvent selection guide for polymer dissolution and can also serve to guide the selection or design of new solvent systems with tuned chemical moieties. However, we note that these ranking results do not assert any absolute conclusion such as which class is always better for dissolution, since ranking classes by what percentage of the top solvents are in each class is not sufficiently comprehensive. For example, the aromatic class ranks quite high for multiple polymers, which can be partially attributed to the fact that it is the most common class (23%) in the solvent library.

**Table 4.** Analysis of functional groups associated with the top solvents for each polymer. Top solvents are defined as those ranked within the top 10% of solvents ranked by solubility and with a minimum predicted solubility of at least 5 wt% at any temperature.

Polymer	EVOH	PE	PP	PS	PET	PVC	Nylon 6	Nylon 66
Number of top solvents	100	100	100	100	95	100	84	49
Top solvent classes	alcohol amine aromatic carboxylic acid amide ether	aromatic ester ether ketone alkene alkane	aromatic alkane ketone ether alkene ester	aromatic ketone alkene ether sulfide	aromatic amine nitrile alkyl halide alkene	ether ketone alcohol amide amine	aromatic carboxylic acid alkyl halide alcohol	carboxylic acid aromatic nitrogen alkene alkyl halide
Example solvents	glycol triethylamine phenol	toluene dibutyl ether 4-heptanone octene	p-xylene cycloheptane 4-heptanone dibutyl ether	styrene toluene cyclohexanone	1-naphthol 3-chloroaniline butyronitrile	1,4-dioxane ethoxyethanol cyclohexanone	2-chlorophenol formic acid chloroform	acrylic acid m-cresol pyrrole

### Polymer separation sequence and solvent screening

A typical STRAP process employs a sequential series of solvent washes with each solvent selected to selectively dissolve a target polymer from the mixture. An important consideration in designing such a process is the sequence in which polymers are dissolved and separated because different separation sequences for the same mixture of polymers lead to different requirements for selectivity. For example, a STRAP process involving sequential dissolution of each component of mixed plastic waste containing 3 polymers can have 6 possible sequences. As noted above, each sequence can impact the selection of solvents (*e.g.*, by leading to a small number of possible options for sequences that target hard-to-dissolve polymers first) and similarly influence process economics and life cycle metrics.

To guide the design of dissolution-based plastic recycling processes and automate solvent screening, we developed a tool to generate all possible sequence and screen suitable solvents for each solvent based on the computational solubility predictions. **Figure 4** shows an example of generating separation sequences for a polymer mixture containing PE, EVOH and PET, which are the constituents of a multilayer plastic packaging film studied in our previous work.<sup>11</sup> The tool first generates all 6 possible separation sequences for the polymer mixture under the assumption that only one polymer is to be selectively dissolved in each step. It then provides ranked lists of solvent candidates for all steps in all separation sequences. For example, in the first separation sequence, EVOH is the first polymer to be dissolved, PE is the second, and PET is then recovered as a residual component that is not dissolved because solvents for its dissolution are rare (**Figure 3**). Step 1 of this sequence requires a solvent that selectively dissolves EVOH but not PE or PET and Step 2 requires a solvent that dissolves PE but not PET. A few top-ranked solvents for each of these steps are shown in **Figure 4** as an example. This ranking is based on the solubility difference between the target polymer and other polymers; detailed criteria are available in the ESI. Each separation sequence has its own selectivity requirements and therefore leads to different sets of eligible solvents. Some separation sequences will have a wide range of solvent candidates, while some sequences have few possible solvents (*e.g.*, when a rarely soluble polymer like PET is the first in the sequence). Our program can thus provide results as input for process simulation and techno-economic

analysis to compare and determine suitable separation sequences and selective solvents. Below, we further demonstrate the applicability of this tool in several experimental case studies.

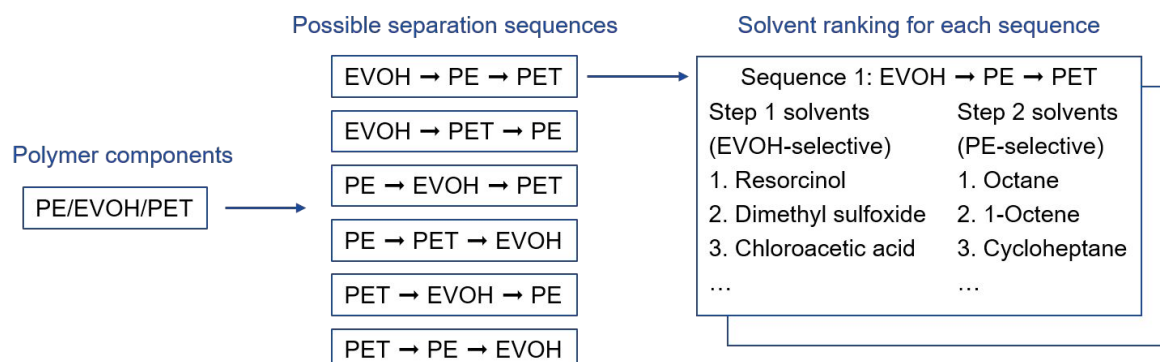


**Figure 4.** An example of generating separation sequences for polymer mixtures.

### Experimental case studies: Separation of binary polymer mixtures

To demonstrate the applicability of our computational approaches in dissolution-based polymer recycling, we perform case studies on the experimental separation of several physical mixtures of polymers. These mixtures include PE/PS, PVC/PET and a 3-component mixture of EVOH/PP/PET which are representative of common real-world plastic products or application scenarios. For example, PE/PS is the composition of a commercial laminated plastic sheet,<sup>56</sup> the PVC/PET mixture represents a typical separation challenge in water bottle recycling processes where PVC is often a contaminant in PET,<sup>57,58</sup> and EVOH/PP/PET can be made into a food packaging material.<sup>59</sup> We use physical mixtures for these case studies to ensure that the system composition is controlled. Our past studies of multilayer plastic packaging materials have demonstrated that computational tools for solubility prediction can be applied to more realistic plastic materials.<sup>11,22,23</sup> We note that the time required for the dissolution of physical mixtures may differ from that of manufactured plastic materials (*e.g.*, multilayer films) that may have components in nanoscale contact, but we focus only on solubility as opposed to dissolution kinetics in this work.

In these case studies, we first select solvents and dissolution temperatures for different mixtures and separation sequences based on computational solubility predictions. To achieve selective dissolution, solvents are selected to have a high solubility for the target polymer and a low solubility for the other polymers in the mixture. As in the prior validation experiments, we preferentially select common laboratory solvents (even if they are not optimal according to computational predictions) to avoid concerns with toxicity. We then conduct experiments to perform the separation of polymers. The separation result is evaluated by the yield and Fourier transform infrared spectroscopy (FTIR) of virgin and recovered resins to confirm resin purity.

The PE/PS mixture is separated in two different sequences. In the first sequence (PE→PS), dodecane at 120 °C is used to selectively dissolve PE but not PS. After 1 h of dissolution, the solid PS is separated by filtering it from the liquid solution of PE. Isopropyl alcohol is then added as a non-solvent (*i.e.*, a solvent with low predicted solubility for the target polymer) to precipitate the PE. **Figure 5** shows photos and FTIR spectra of the virgin and recovered resins. The physical morphologies of the recovered resins change due to the dissolution and precipitation processes, as shown in the photos; the PE resin changes from pellets to flakes while the PS resin changes from a powder to a chunk. However, the FTIR

spectra of the recovered resins are highly consistent with the virgin ones, indicating that the chemical structures of the polymers remain unaffected and that the recovered resins each contain a single polymer component as expected. The yields of the recovered PE and PS are 99.18% and 99.96%, respectively. In the other separation sequence, ethyl acetate is used to selectively dissolve PS, and isopropyl alcohol is used for precipitation. Changing the order of dissolution leads to different yields of 100.21% of PE and 93.84% of PS (**Table 5**). FTIR analysis further indicates that the recovered resins are similar to the virgin resins (**SI Figure S3**). This example shows how separation sequence impacts the performance of the dissolution-based recycling process.

Similar experiments and analysis were performed for the PVC/PET mixture. Only one separation sequence (PVC→PET) was experimentally tested because the other sequence involves the selective dissolution of PET, which has a very limited number of solvent candidates, and most of them are quite uncommon and hazardous (*e.g.*, hexafluoro-2-propanol). **Table 5** summarizes the selected solvents and conditions with corresponding photos and FTIR spectra available in the ESI. We obtain over 90% yield of both polymers using THF as a selective solvent at a relatively low temperature (65 °C), which eliminates concerns with thermal degradation and the production of potentially hazardous products from PVC.<sup>60, 61</sup>

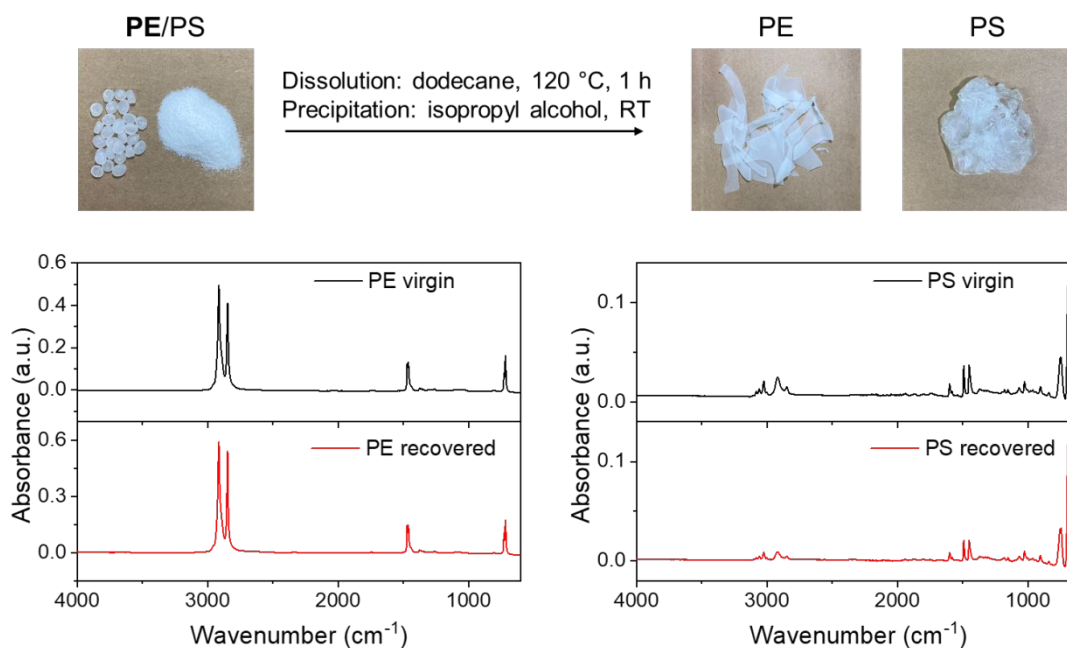


**Figure 5.** Results from the separation of physical mixtures of PE and PS via selective dissolution. The separation sequence is PE→PS. Dodecane at 120 °C is used to selectively dissolve PE. FTIR spectrum verified the purity of both recovered polymers.

**Table 5.** Results from all separation case studies. Additional FTIR spectra and images of resins before and after dissolution are reported in the ESI.

Polymer mixture	Separation sequence	Selective solvent	Temperature and time	Precipitation	Recovery yield
PE/PS	PE→PS	Dodecane (PE)	120 °C 1 h	Non-solvent: isopropyl alcohol	PE: 99.18 % PS: 99.96%
	PS→PE	Ethyl acetate (PS)	75 °C 20 min	Non-solvent: isopropyl alcohol	PE: 100.21% PS: 93.84%
PVC/PET	PVC→PET	THF (PVC)	65 °C 2 h	Non-solvent: water	PVC: 90.61% PET: 94.25%
EVOH/PP/PET	EVOH→PP →PET	EG (EVOH) THP (PP)	120 °C, 1 h 88 °C, 1.5 h	Evaporation	EVOH: 97.6% PP: 78.3% PET: 100.95%
	PP→EVOH →PET	THP (PP) EG (EVOH)	88 °C, 1 h 120 °C, 2 h	Evaporation	EVOH: 98.61% PP: 96.77% PET: 94.23%

**Experimental case study: Separation of ternary polymer mixtures**

For the 3-component mixture (EVOH/PP/PET), we first study the separation sequence EVOH→PP→PET, in which ethylene glycol (EG) is used as an EVOH-selective solvent in the first step, then tetrahydropyran (THP) is used as the PP-selective solvent in the second step. With this sequence, it was found that the yield of PP is low (78.3%) and we observe an undissolved solid which clearly differs from the PET resin. Photos and FTIR spectra of the undissolved solid are included in the ESI. The FTIR spectra suggest that the undissolved solid is a mixture of PP and EVOH. We speculate that some EVOH and PP agglomerate in the presence of EG at the first step and remain undissolved throughout the remaining selective dissolution process. Therefore, a different separation sequence (PP→EVOH→PET) was tested with the same solvents and temperatures. In this sequence, PP is the first to be separated to avoid its contact with EG. With this sequence, we observe no undissolved solid and the yields for all three polymers are excellent (>94%, **Table 5**). This example shows how unexpected effects can arise during selective dissolution processes to further demonstrate the value of assessing alternative separation sequences.

There are multiple other possible separation sequences for this 3-polymer mixture EVOH/PP/PET. We did not test all sequences experimentally, but instead propose some applicable solvent selections here. **Table 6** presents four more separation strategies for this



polymer mixture. In these strategies, we specifically focus on enabling temperature-controlled precipitation, in which a target polymer is dissolved at a high temperature and precipitated at a low temperature (as opposed to being precipitated through addition of a non-solvent). Temperature-controlled precipitation has been shown to be preferred in STRAP processes based on prior techno-economic analysis.<sup>17, 22</sup> We selected solvents from those that satisfy the following rules: the predicted solubility of the polymer to be dissolved must be greater than 5 wt% while the solubility of other polymers must be lower than 3 wt%, the difference in the predicted solubilities must be greater than 5 wt% to achieve selectivity, and the predicted solubility of the dissolved polymer at room temperature must be 80% lower than its solubility at high temperature to assure the feasibility of temperature-controlled precipitation. **Figure 6** provides an illustrative example of the workflow of the first proposed separation strategy, in which EVOH is first dissolved in resorcinol and PET is then dissolved in pyrrole. These examples demonstrate the capability of the computational methods to rapidly generate potential separation sequences for further evaluation experimentally or as input for further techno-economic/life cycle analysis.

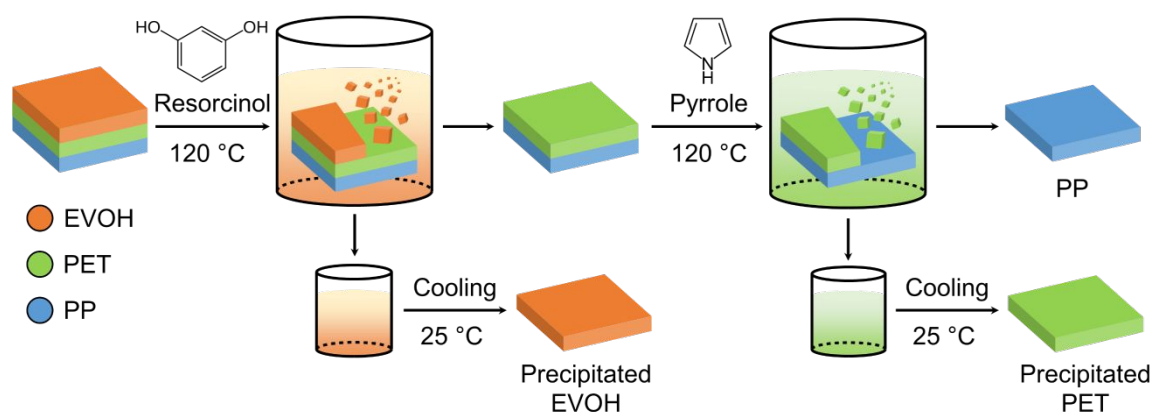


**Figure 6.** Schematic of a proposed separation process for the PP/EVOH/PET mixture using solvents and temperatures optimized for selective dissolution.

**Table 6.** Examples of other possible separation strategies for PP/EVOH/PET mixture. Selective solvents and the corresponding solubility predictions are listed for 4 different separation sequences. Each solvent selectively dissolves a target polymer at a high temperature and precipitates the polymer at room temperature.

Separation sequence	Predicted solubilities			
	Solvent	Polymer	T (°C)	Solubility (wt%)
EVOH→PET→PP	Resorcinol	EVOH	120	31.2
		PET	25	3.7
		PP	120	2.2
	Pyrrole	PET	120	15.8
		PP	25	0.1
		PP	120	1.3
PP→PET→EVOH	Cycloheptane	PP	117	44.7
		PET	25	3.0
		EVOH	117	0.0
	Methyl isothiocyanate	PET	118	19.8
		EVOH	25	0.1
		EVOH	118	1.6
PET→PP→EVOH	Propionitrile	PET	96	9.1
		PP	25	0.1
		EVOH	96	1.4
	1-Octene	PP	96	2.0
		PP	120	42.0
		EVOH	25	2.3
PET→EVOH→PP	Dibromomethane	EVOH	120	0.1
		PET	96	6.9
		PET	25	0.4
	DMSO	EVOH	96	0.1
		PP	96	0.5
		EVOH	120	35.3
		PP	25	1.3
		PP	120	1.7

## Conclusions

In this work, we established a computational workflow for guiding the design of dissolution-based polymer recycling processes using large-scale, temperature-dependent polymer solubility predictions. Our method integrates MD simulations, conformational sampling, COSMO-RS calculations, as well as experimental calibration. Using MD simulations, we modeled polymers as oligomers in dilute solution and selected representative conformers from the resulting MD trajectories. These conformers, along with an experimentally measured solubility in a reference solvent, were input to COSMO-RS solid-liquid equilibrium

calculations to predict polymer solubilities in numerous solvents. We established a solubility database for 8 polymers and 1007 solvents at multiple temperatures and experimentally verified computational predictions for a selected subset of systems. Based on the database, we studied the relationship between polymers and their top solvents via functional group analysis of solvent molecular structures. We further developed a computational tool to automatically select suitable solvents for sequential selective dissolution-based plastic recycling processes (like the STRAP process) while evaluating all possible separation sequences. We demonstrated the applicability of the method using multiple experimental case studies in which physical mixtures of polymers were successfully separated via sequential selective dissolution. This computational approach thus has promise for guiding the design of STRAP processes for multicomponent plastic waste, and could further be used to optimize existing STRAP processes by selecting alternative solvents (*e.g.*, green solvents).

While the approach in this work was demonstrated for sequential selective dissolution processes in which only one polymer was dissolved at each step, future work will continue to develop a combinatorial optimization model that allows for the dissolution of multiple polymers at a time in order to search for the best separation sequence of a STRAP process. The model will also account for factors such as the densities of solvents and the percentage of each polymer in the waste stream when considering challenges that may be faced while scaling up dissolution-based processes. We will further combine these models with technoeconomic analysis and life-cycle assessment tools to evaluate the comprehensive impact of solvents and identify tradeoffs between possible separation sequences, which will facilitate the design of economically feasible and environmentally friendly STRAP processes. Finally, we envision further expanding the database to consider new classes of green or designer solvents with potential value in polymer dissolution, such as ionic liquids or deep eutectic solvents.<sup>62, 63</sup>

### **Conflicts of Interest**

There are no conflicts of interest to declare.

### **Acknowledgements**

This material is based upon work supported by the U.S. Department of Energy, Office of Energy Efficiency and Renewable Energy, Bioenergy Technologies Office under Award Number DE-EE0009285. The authors would also like to thank Kevin Nelson, Daniel Miller and Steven Grey from Amcor Flexibles for providing polymer samples and helpful insights in the experiments.

## References

1. T. M. Letcher, *Plastic waste and recycling: environmental impact, societal issues, prevention, and solutions*, Academic Press, 2020.
2. United Nations Environment Programme, *From Pollution to Solution: A Global Assessment of Marine Litter and Plastic Pollution*, 2021.
3. J. M. Garcia and M. L. Robertson, *Science*, 2017, **358**, 870-872.
4. O. Horodytska, F. J. Valdés and A. Fullana, *Waste Manage. (Oxford)*, 2018, **77**, 413-425.
5. C. Jehanno, J. W. Alty, M. Roosen, S. De Meester, A. P. Dove, E. Y.-X. Chen, F. A. Leibfarth and H. Sardon, *Nature*, 2022, **603**, 803-814.
6. D. Lithner, Å. Larsson and G. Dave, *Sci. Total Environ.*, 2011, **409**, 3309-3324.
7. J. K. Kim, S. Thomas and P. Saha, *Multicomponent Polymeric Materials*, Springer, 2016.
8. L. K. Massey, *Permeability properties of plastics and elastomers: a guide to packaging and barrier materials*, Cambridge University Press, 2003.
9. C. T. de Mello Soares, M. Ek, E. Östmark, M. Gällstedt and S. Karlsson, *Resources, Conservation and Recycling*, 2022, **176**, 105905.
10. A. Mieth, E. Hoekstra and C. Simoneau, *European Commission JRC Technical reports*, 2016.
11. T. W. Walker, N. Frelka, Z. Shen, A. K. Chew, J. Banick, S. Grey, M. S. Kim, J. A. Dumesic, R. C. Van Lehn and G. W. Huber, *Sci. Adv.*, 2020, **6**, eaba7599.
12. U.S. Environmental Protection Agency, *Plastics: Material-Specific Data*, <https://www.epa.gov/facts-and-figures-about-materials-waste-and-recycling/plastics-material-specific-data>, (accessed May 1, 2022).
13. H. Li, H. A. Aguirre-Villegas, R. D. Allen, X. Bai, C. H. Benson, G. T. Beckham, S. L. Bradshaw, J. L. Brown, R. C. Brown, V. S. Cecon, J. B. Curley, G. W. Curtzwiler, S. Dong, S. Gaddameedi, J. E. García, I. Hermans, M. S. Kim, J. Ma, L. O. Mark, M. Mavrikakis, O. O. Olafasakin, T. A. Osswald, K. G. Papanikolaou, H. Radhakrishnan, M. A. Sanchez Castillo, K. L. Sánchez-Rivera, K. N. Tumu, R. C. Van Lehn, K. L. Vorst, M. M. Wright, J. Wu, V. M. Zavala, P. Zhou and G. W. Huber, *Green Chem.*, 2022, **24**, 8899-9002.
14. S. Billiet and S. R. Trenor, *ACS Macro Letters*, 2020, **9**, 1376-1390.
15. J. G. Poulakis and C. D. Papaspyrides, *Adv. Polym. Tech.*, 1995, **14**, 237-242.
16. D. Triebert, H. Hanel, M. Bundt and K. Wohnig, in *Circular Economy of Polymers: Topics in Recycling Technologies*, ACS Publications, 2021, pp. 33-59.
17. A. del Carmen Munguía-López, D. Göreke, K. L. Sánchez-Rivera, H. A. Aguirre-Villegas, S. Avraamidou, G. Huber and V. M. Zavala, *Green Chem.*, 2023, **25**, 1611-1625.
18. S. Ügdüler, K. M. Van Geem, M. Roosen, E. I. Delbeke and S. De Meester, *Waste Manage. (Oxford)*, 2020, **104**, 148-182.
19. I. Vollmer, M. J. Jenks, M. C. Roelands, R. J. White, T. van Harmelen, P. de Wild, G. P. van Der Laan, F. Meirer, J. T. Keurentjes and B. M. Weckhuysen, *Angew. Chem. Int. Ed.*, 2020, **59**, 15402-15423.
20. A. Schwarz, T. Ligthart, D. G. Bizarro, P. De Wild, B. Vreugdenhil and T. Van Harmelen, *Waste Manage. (Oxford)*, 2021, **121**, 331-342.
21. D. Maga, M. Hiebel and N. Thonemann, *Resources, Conservation and Recycling*, 2019, **149**, 86-96.
22. K. L. Sánchez-Rivera, P. Zhou, M. S. Kim, L. D. González Chávez, S. Grey, K. Nelson, S. C. Wang, I. Hermans, V. M. Zavala, R. C. Van Lehn and G. W. Huber, *ChemSusChem*, 2021, **14**, 4317-4329.
23. K. L. Sánchez-Rivera, A. del Carmen Munguía-López, P. Zhou, V. S. Cecon, J. Yu, K. Nelson, D. Miller, S. Grey, Z. Xu, E. Bar-Ziv, K. L. Vorst, G. W. Curtzwiler, R. C. Van Lehn, V. M. Zavala and G. W. Huber, *Submitted (Available at SSRN 4355723)*, 2022.
24. D. R. Bloch, *The Wiley Database of Polymer Properties*, 2003.
25. Y.-B. Zhao, X.-D. Lv and H.-G. Ni, *Chemosphere*, 2018, **209**, 707-720.
26. J. H. Hildebrand, *Proc. Natl. Acad. Sci. U. S. A.*, 1950, **36**, 7.
27. C. M. Hansen, *Hansen solubility parameters: a user's handbook*, CRC press, 2007.
28. R. W. Taft, J.-L. M. Abboud, M. J. Kamlet and M. H. Abraham, *J. Solution Chem.*, 1985, **14**, 153-186.

29. V. Gutmann, *Electrochim. Acta*, 1976, **21**, 661-670.
30. C. G. Swain, M. S. Swain, A. L. Powell and S. Alunni, *J. Am. Chem. Soc.*, 1983, **105**, 502-513.
31. S. Abbott and C. M. Hansen, *Hansen solubility parameters in practice*, Hansen-Solubility, 2008.
32. A. Chandrasekaran, C. Kim, S. Venkatram and R. Ramprasad, *Macromolecules*, 2020, **53**, 4764-4769.
33. P. Zhou, K. L. Sánchez-Rivera, G. W. Huber and R. C. Van Lehn, *ChemSusChem*, 2021, **14**, 4307-4316.
34. F. P. Byrne, S. Jin, G. Paggiola, T. H. Petchey, J. H. Clark, T. J. Farmer, A. J. Hunt, C. R. McElroy and J. Sherwood, *Sustainable Chem. Processes*, 2016, **4**, 1-24.
35. R. G. Dastidar, M. S. Kim, P. Zhou, Z. Luo, C. Shi, K. J. Barnett, D. J. McClelland, E. Y.-X. Chen, R. C. Van Lehn and G. W. Huber, *Green Chem.*, 2022.
36. M. J. Abraham, T. Murtola, R. Schulz, S. Páll, J. C. Smith, B. Hess and E. Lindahl, *SoftwareX*, 2015, **1**, 19-25.
37. J. Wang, W. Wang, P. A. Kollman and D. A. Case, *J. Mol. Graphics Modell.*, 2006, **25**, 247-260.
38. J. Wang, R. M. Wolf, J. W. Caldwell, P. A. Kollman and D. A. Case, *J. Comput. Chem.*, 2004, **25**, 1157-1174.
39. J. Li, C. T. Maravelias and R. C. Van Lehn, *Ind. Eng. Chem. Res.*, 2022, **61**, 9025-9036.
40. M. Frisch, G. Trucks, H. Schlegel, G. Scuseria, M. Robb, J. Cheeseman, G. Scalmani, V. Barone, G. Petersson and H. Nakatsuji, *Journal*, 2016.
41. A. Klamt, *J. Phys. Chem.*, 1995, **99**, 2224-2235.
42. A. Klamt, V. Jonas, T. Bürger and J. C. Lohrenz, *J. Phys. Chem. A*, 1998, **102**, 5074-5085.
43. J. Kahlen, K. Masuch and K. Leonhard, *Green Chem.*, 2010, **12**, 2172-2181.
44. COSMOlogic GmbH & Co KG, 2019.
45. B. Wunderlich, *Thermal Analysis*, Academic Press, San Diego, CA, 1990.
46. P. Warangkhanana and M. Rathanawan, 2015.
47. F. Eckert and A. Klamt, *AIChE J.*, 2002, **48**, 369-385.
48. A. Klamt, F. Eckert, M. Hornig, M. E. Beck and T. Bürger, *J. Comput. Chem.*, 2002, **23**, 275-281.
49. COSMOlogic GmbH & Co KG, *Journal*, 2019.
50. V. S. Cecon, G. W. Curtzwiler and K. L. Vorst, *Macromolecular Materials and Engineering*, 2022, 2200346.
51. J. Sun, D. Liu, R. P. Young, A. G. Cruz, N. G. Isern, T. Schuerg, J. R. Cort, B. A. Simmons and S. Singh, *ChemSusChem*, 2018, **11**, 781-792.
52. J. Poulakis and C. Papaspyrides, *J. Appl. Polym. Sci.*, 2001, **81**, 91-95.
53. D. Weininger, *Journal of chemical information and computer sciences*, 1988, **28**, 31-36.
54. Daylight Chemical Information Systems, SMARTS - A Language for Describing Molecular Patterns, <https://www.daylight.com/dayhtml/doc/theory/theory.smarts.html>, (accessed May 1, 2022).
55. G. Landrum, Rdkit: Open-source cheminformatics software, <https://www.rdkit.org/>, (accessed May 1, 2022).
56. Desu Technology, Laminated Plastic Sheet PS-PE, <https://desuplastic.com/laminated-plastic-sheet/ps-pe/>, (accessed May 1, 2022).
57. M. T. Brouwer, F. Alvarado Chacon and E. U. Thoden van Velzen, *Packaging Technology and Science*, 2020, **33**, 373-383.
58. ASG Recycling, PVC in PET Bottle Recycling, <https://www.petbottlewashingline.com/pvc-in-pet-bottle-recycling/>, (accessed May 1, 2022).
59. ROL, PET EVOH PP, <https://www.rol-italy.com/en/product/pet-evoh-pp/>, (accessed May 1, 2022).
60. R. Miranda, H. Pakdel, C. Roy and C. Vasile, *Polym. Degrad. Stab.*, 2001, **73**, 47-67.
61. I. C. McNeill, L. Memetea and W. J. Cole, *Polym. Degrad. Stab.*, 1995, **49**, 181-191.
62. Z. Sumer and R. C. Van Lehn, *ACS Sustainable Chem. Eng.*, 2022, **10**, 10144-10156.
63. M. Mohan, J. D. Keasling, B. A. Simmons and S. Singh, *Green Chem.*, 2022, **24**, 4140-4152.